Journal of Medicinal Chemistry

Novel Allosteric Activators for Ferroptosis Regulator Glutathione Peroxidase 4

Cong Li, Xiaobing Deng, Weilin Zhang, Xiaowen Xie, Marcus Conrad, Ying Liu, José Pedro Friedmann Angeli, and Luhua Lai

J. Med. Chem., **Just Accepted Manuscript** • Publication Date (Web): 24 Apr 2018

Just Accepted

ACS Publications

is published by the American Chemical Society. 1155 Sixteenth Street N.W., Washington, DC 20036

Novel Allosteric Activators for Ferroptosis Regulator Glutathione Peroxidase 4

Cong Li,[†,&] *Xiaobing Deng,*[∥,&] *Weilin Zhang,*[†] *Xiaowen Xie,*[‡] *Marcus Conrad,*[§] *Ying Liu,*[†,‡] *José Pedro Friedmann Angeli*,*[#] *and Luhua Lai**[†,∥,‡]

[†]BNLMS, State Key Laboratory for Structural Chemistry of Unstable and Stable Species, College of Chemistry and Molecular Engineering, [∥]Peking-Tsinghua Center for Life Sciences, and [‡]Center for Quantitative Biology, Peking University, Beijing 100871, China

[§]Institute of Developmental Genetics, Helmholtz Zentrum München, 85764 Neuherberg, Germany

[#]Rudolf Virchow Center for Experimental Biomedicine, University of Würzburg, 97080 Würzburg, Germany

&Co-first authors

ABSTRACT: Glutathione peroxidase 4 (GPX4) is essential for cell membrane repair, inflammation suppression, and ferroptosis inhibition. GPX4 upregulation provides unique drug discovery opportunities for inflammation and ferroptosis-related diseases. However, rational design of protein activators is challenging. Until now, no compound has been reported to activate the enzyme activity of GPX4. Here, we identified a potential allosteric site in GPX4, and

successfully found eight GPX4 activators using a novel computational strategy and experimental studies. Compound **1** from the virtual screen increased GPX4 activity, suppressed ferroptosis, reduced pro-inflammatory lipid mediator production, and inhibited NF-κB pathway activation. Further chemical synthesis and structure-activity relationship studies revealed seven more activators. The strongest compound **1d4** increased GPX4 activity to 150 % at 20 μM in cell-free assay and 61 μM in cell extracts. Therefore, we demonstrated that GPX4 can be directly activated using chemical compounds to suppress ferroptosis and inflammation. Meanwhile, the discovery of GPX4 activators verified the possibility of rational design of allosteric activators.

INTRODUCTION

Glutathione peroxidase 4 (GPX4) is the sole antioxidant enzyme that repairs lipid hydroperoxides, regulates eicosanoid biosynthesis, cytokine signaling,[1] and ferroptosis.[2] Activating GPX4 is a promising strategy to suppress eicosanoid generation and inflammation,[3-5] whereas GPX4 insufficiency triggers ferroptosis—a non-apoptotic form of cell death characterized by increased lipid hydroperoxide levels.[2,6,7] Ferroptosis has attracted considerable attention due to its implication in ischemia reperfusion injury and neurodegeneration.[8] Ferroptosis suppression requires GPX4 peroxidase activity, which is responsible for prevention of arachidonoyl and adrenoyl phosphatidylethanolamines peroxidized species formation.[9] Several compounds that can inhibit ferroptosis and the eicosanoid storm generated during its execution have been developed. The ferroptosis suppression strategies that have been used can be divided into three groups: 1) suppression of lipid peroxidation using radical trapping antioxidants,[10] 2) decrease of esterified polyunsaturated fatty acids such as arachidonic and

adrenic acid through acyl-CoA synthetase long-chain family member 4 (ACSL4) inhibition,[11] or 3) lipoxygenase (LOX) inhibition.[12] As previous studies suggest GPX4 activation suppresses lipid peroxidation generated by lipoxygenase enzymes,[3-5] we rationalized that an alternative way to suppress cell death and the eicosanoids formed during ferroptosis would be through increasing GPX4 peroxidase activity.

However, small molecule activator discovery is a much more challenging task than inhibitor discovery. Many inhibitors that bind to the substrate pockets of protein targets have been identified, whereas most activators function by allosteric regulation. However, allosteric site information is lacking for most enzymes, including GPX4. To date, the most commonly used method for identifying activators relies on laborious high-throughput experimental screening.[13] Therefore, a rational approach for discovering activators is urgently needed.[14,15]

In this study, we used a rational strategy to discover GPX4 allosteric activators. We first computationally identified a potential allosteric site using ligand-binding site detection and motion correlation analysis for allosteric site prediction. We then used this predicted site to virtually screen a chemical library to identify potential GPX4 activators. Our initial enzyme assay screen identified one GPX4 activating compound. We demonstrated this GPX4 activator could inhibit ferroptosis and suppress the generation of pro-inflammatory lipid mediators in cell assays. This compound was further optimized using chemical synthesis and structure-activity relationship (SAR) analysis.

RESULTS AND DISCUSSION

Allosteric Site Prediction and Virtual Screening. To find suitable binding pockets for designing allosteric activators, we first used the binding site detection program CAVITY[16,17] to

identify surface cavities in the crystal structure of human GPX4 U46C mutant (hGPX4-C, PDB entry 2OBI[18]). These surface cavities were analyzed using the CorrSite method based on the motion correlation between potential ligand- and substrate-binding sites that we developed recently.[19] This procedure predicted one allosteric site localized on the opposite side of the substrate-binding site (Figure 1a), and the two sites were separated by the central β-sheet consisting of five β-strands. The predicted potential allosteric site has the highest CAVITY score and a CorrSite score of 1.49 (cavities with CorrSite score > 0.5 were predicted as potential allosteric sites in the CorrSite method which was developed based on a list known allosteric proteins). The volume of the olive-shaped allosteric site is 278.4 $Å^3$ with a predicted maximal pKd of 7.48. We performed molecular dynamics simulations to analyze the dynamic changes of the predicted allosteric site, and confirmed that this site was persistent in volume with high motion correlations with the substrate-binding site (Supporting Information, Figure S1). The allosteric site is surrounded by three acidic residues (D21, D23, and D101), two basic residues (K31 and K90), and seven apolar residues (I22, A93, A94, V98, F100, M102, and F103).

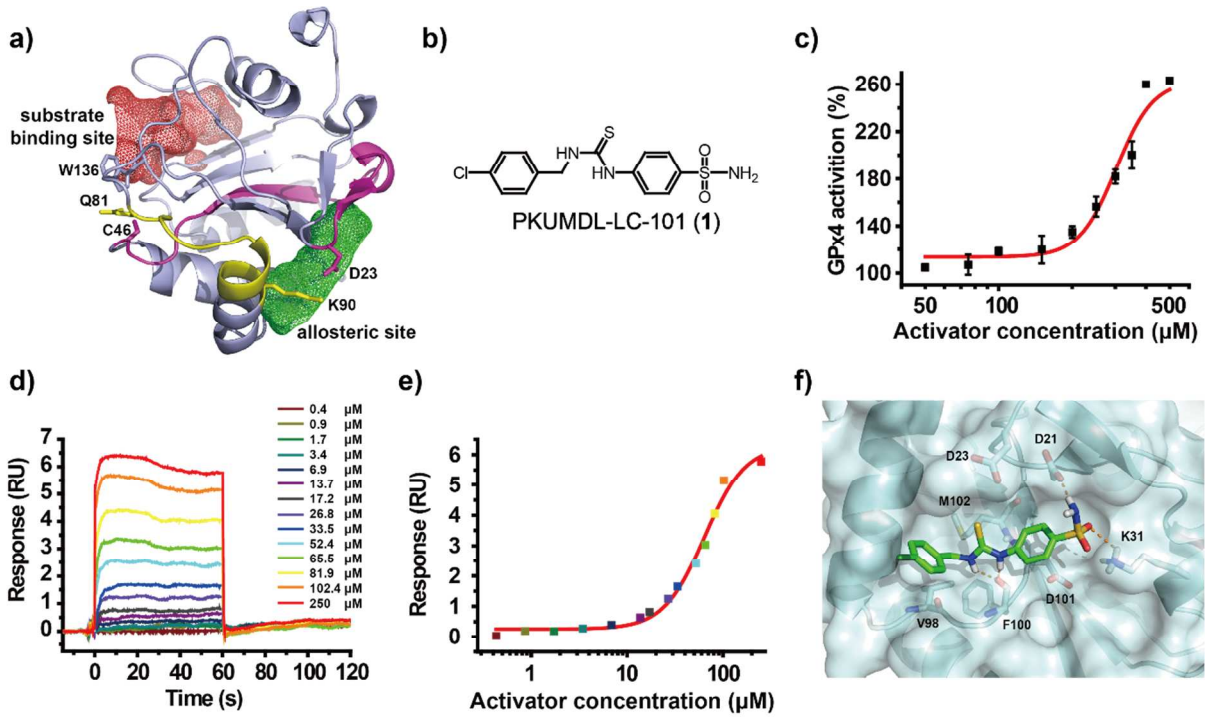

Figure 1. GPX4 activator identification. a) The predicted allosteric site (shown in green) using CAVITY and CorrSite is on the opposite side from the substrate-binding site (shown in red) across the protein (PDB entry 2OBI[18]). The connections between D23 and C46, and K90 and Q81 are shown in magentas and yellow respectively. b) Chemical structure of **1**. c) Dose-response curve for **1** in cell-free assays. Data shown represent the mean ± SEM (n = 6). d) SPR dose-response curves of **1**. e) Data in Figure 1d at equilibrium were fitted with the Hill model. The color of the dots are consistent with the color of the response curves in Figure 1d (K_D = 63 ± 5 μM). f) Predicted binding mode of **1**. The hydrogen bonds between the activator (green) and GPX4 (pale cyan, PDB entry 2OBI[18]) are shown as dashed orange lines.

We then used the molecular docking program Glide to virtually screen against the SPECS compounds library (pan assay interference compounds[20] excluded). After performing a two-step

molecular docking scheme, we selected 251 compounds for experimental testing according to the following criteria: compounds should have good interactions with pocket residues with (1) at least one hydrogen bond, and (2) good hydrophobic interactions (see Experimental Section).

Biological Evaluation. *Cell-Free Enzyme Activity Assay.* The activating activities of the 251 selected compounds were tested in the cell-free assay. Compound PKUMDL-LC-101 (**1**) (Figure 1b) increased the hGPX4-C enzymatic activity in a dose-dependent manner (Figure 1c) to 263 % of the original enzyme activity. Compound **1** was shown to directly bind to hGPX4-C using the surface plasmon resonance (SPR) assay, with 63 ± 5 μM dissociation constant (Figure 1d and Figure 1e).

Prevention of Erastin-Induced Ferroptosis. Activating GPX4 may be beneficial during erastin (Era) induced ferroptosis. We tested whether **1** can prevent Era-induced ferroptosis in human HT-1080 fibrosarcoma cells.[2] We incubated the cells with **1** and subjected them to Era (10 μM) treatment. After 24 hours, cell viability was determined using the MTS assay (Figure 2a). Compound **1** could inhibit Era-induced ferroptosis, thus supporting the use of GPX4 activator as antiferroptotic agent.

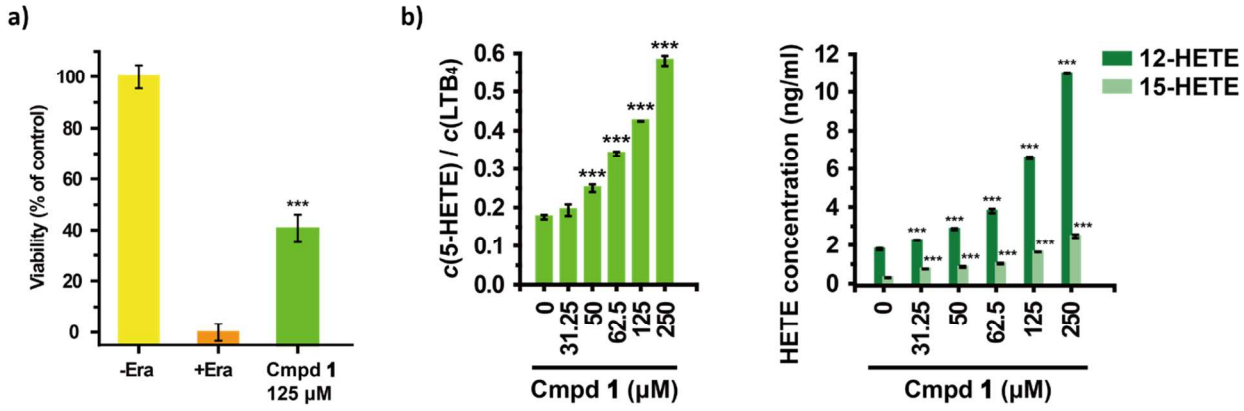

Figure 2. The effects of **1** in cellular model of erastin-induced ferroptosis and human PMN assay. a) Prevention of erastin-induced ferroptosis by GPX4 activator **1** in HT-1080 cells. Compound **1** prevented cell death with a lethal concentration of erastin (Era, 10 μM). Data shown represent the mean ± SEM (n = 5). b) Dose-dependent GPX4 activation in PMN cells. Data shown represent the mean ± SEM (n = 4). The statistical significance was determined using a two-tailed t-test, ***$p < 0.001$.

Influence on Eicosanoid Biosynthesis. During the course of ferroptosis, arachidonic acid (AA) oxidation products are released,[7] which may drive a secondary inflammatory damage in ferroptosis-related pathologies. In the inflammation-related AA metabolic network, AA is oxidized to 5-HpETE, 12-HpETE, and 15-HpETE by 5-LOX, 12-LOX, and 15-LOX, respectively (Supporting Information, Figure S2).[21] GPX4 converts HpETEs to the corresponding HETEs. And stimulating the release of these anti-inflammatory lipid mediators is an additional beneficial effect of GPX4 activators. Thus, we tested the effects of **1** on eicosanoid biosynthesis using human polymorphonuclear leucocytes (PMN). We used this assay to assess the eicosanoids formation without interference from cell death. We stimulated the 5-LOX pathway using calcium ionophore A23187[22,23] and used LC-MS/MS to detect the formation of major eicosanoids derived from AA. Compound **1** induced GPX4 activating effects in a dose-dependent manner including an increased 5-HETE/leukotriene B_4 (LTB_4) ratio, 12-HETE level, and 15-HETE level (Figure 2b and Supporting Information Figure S3). To confirm that **1** does not affect the other enzymes in the AA network, we tested the effects of **1** on cyclooxygenase 1 (COX-1), cyclooxygenase 2 (COX-2), microsomal prostaglandin E_2 synthase 1 (mPGES-1), 5-LOX, leukotriene A4 hydrolase (LTA_4H), 12-LOX, and 15-LOX. Compound **1** did not show

activity against COX-1, COX-2, 5-LOX, 12-LOX, or 15-LOX, and only slightly inhibited mPGES-1 and LTA_4H (inhibition = 23 % and 17 % at 500 μM, respectively).

Inhibition of the NF-κB Pathway. To further demonstrate that GPX4 activator can modulate GPX4-mediated events, we tested its effect in cytokine signaling. Direct involvement of hydrogen peroxide in NF-κB activation has been discussed,[24] and GPX4 might prevent the TNF or IL-1 mediated NF-κB activation.[25,26] We used the dual-luciferase reporter assay system to test the effects of **1** on TNF or IL-1 induced activation of NF-κB pathway in HEK293T cells. Compound **1** inhibited the TNF and IL-1 induced NF-κB pathway activation dose-dependently (Figure 3).

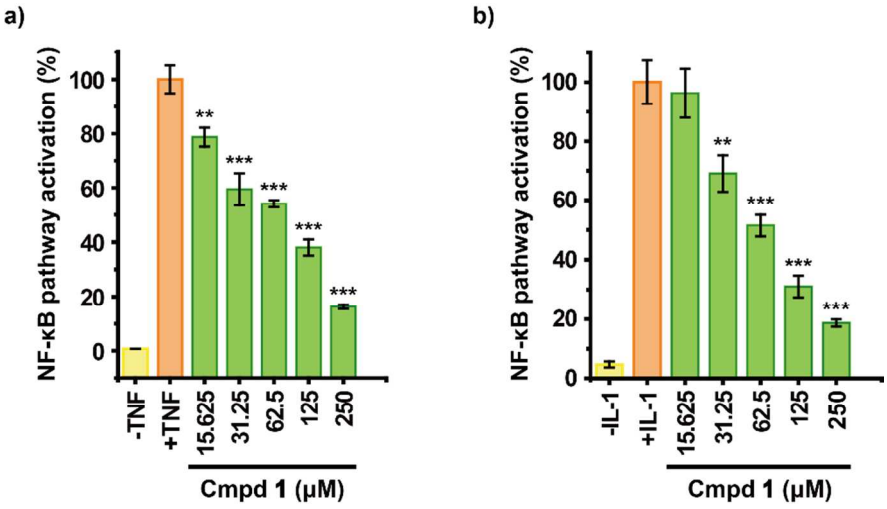

Figure 3. Dose-dependent inhibition of NF-κB pathway activation by GPX4 activator. a) Inhibition of TNF induced NF-κB pathway activation. b) Inhibition of IL-1 induced NF-κB pathway activation. Data shown represent the mean ± SEM (n = 5). The statistical significance was determined using a two-tailed t-test, $^{**}p < 0.01$, $^{***}p < 0.001$.

Structure−Activity Relationship. The binding mode of **1** was predicted by molecular docking studies (Figure 1f). To establish the SAR for the GPX4 activator, several analogues of **1** were tested. Three compounds (**1s1**, **1s2**, and **1s3**) retained the capacity to increase GPX4 activity in a concentration-dependent manner in the cell-free assay (Table 1 and Supporting Information Figure S4). As a general feature, compounds with a bulkier R^1 group were less potent. To further explore the SAR of **1**, we designed and synthesized 12 analogues (Scheme 1, see Experimental Section for details) and tested their effects on cell-free GPX4 enzyme activity (Table 1 and Supporting Information Figure S5).

Table 1. Activity of 1 analogues[a]

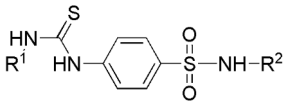

Cmpd	Name	R^1	R^2	Max. activation	Conc. required to reach 150 % activation (μM)	Activation with 200 μM of compound
1	PKUMDL-LC-101	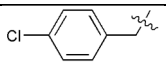	H	263 %	248	127 %
1s1	PKUMDL-LC-101-S01	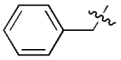	H	300 %	255	129 %
1s2	PKUMDL-LC-101-S02	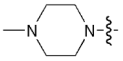	H	200 %	285	115 %
1s3	PKUMDL-LC-101-S03		H	225 %	147	167 %
1d1	PKUMDL-	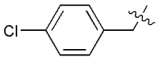	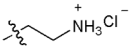	activation with 200 μM		

	LC-101-D01				of compound < 115 %	
1d2	PKUMDL-LC-101-D02				activation with 200 μM of compound < 115 %	
1d3	PKUMDL-LC-101-D03			437 %	29	318 %
1d4	PKUMDL-LC-101-D04			279 %	20	219 %
1d5	PKUMDL-LC-101-D05				activation with 200 μM of compound < 115 %	
1d6	PKUMDL-LC-101-D06				activation with 200 μM of compound < 115 %	
1d7	PKUMDL-LC-101-D07				activation with 200 μM of compound < 115 %	
1d8	PKUMDL-LC-101-D08				activation with 200 μM of compound < 115 %	
1d9	PKUMDL-LC-101-D09				activation with 200 μM of compound < 115 %	
1d10	PKUMDL-LC-101-D10			209 %	121	167 %
1d11	PKUMDL-LC-101-D11			214 %	301	121 %
1d12	PKUMDL-LC-101-D12				activation with 200 μM of compound < 115 %	

[a]All measurements were performed in hextuplicate. Data were given by reading corresponding values from the curves fitted using the Hill model.

Scheme 1. Synthesis Procedures for the 1 Analogues

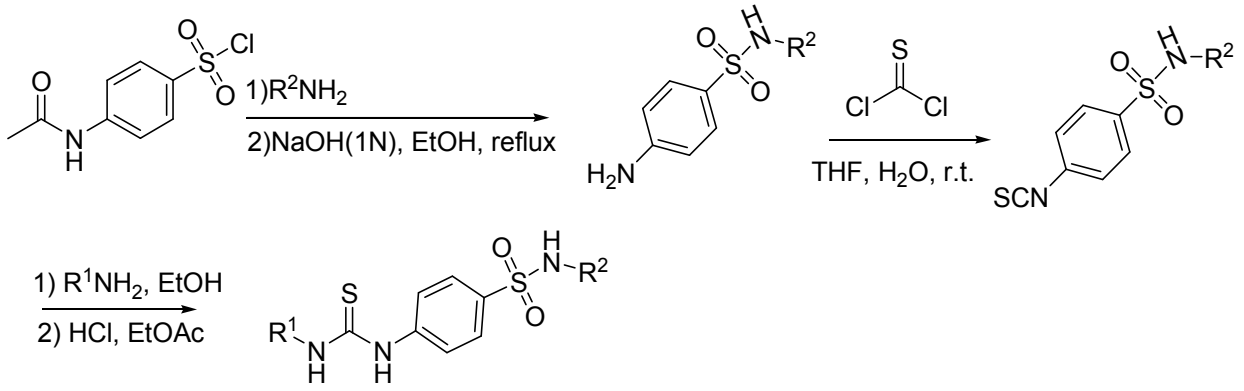

Since the negatively charged residues D21 and D23 in the allosteric site located near the R^2 group, we designed compounds with positively charged substitution on the sulfonamide amino group to enhance the ligand-target interactions by an additional salt bridge. Compounds **1d1**, **1d2**, **1d3**, **1d4**, **1d5**, and **1d6** with 2-aminoethyl R^2 group have different sizes of R^1 groups, including 4-chlorobenzyl, ethyl, *tert*-butyl, cyclopentyl, cyclohexyl, and cycloheptyl. Among them, *tert*-butyl (**1d3**) and cyclopentyl (**1d4**) R^1 groups improved the activity, and the other R^1 groups larger than cyclopentyl or smaller than *tert*-butyl were less potent, confirming that steric effect is crucial and subtle in the binding to the small allosteric site. Compound **1d4** enhanced GPX4 activity to 279 %. The **1d4** concentration required to activate the enzyme activity to 150 % was approximately one order of magnitude lower than that of **1** (20 μM vs 248 μM). The dissociation constant of compound **1d4** determined by SPR assay (Supporting Information, Figure S6) was also lower than that of **1** (19 ± 1 μM vs 63 ± 5 μM).

We also explored other R^2 groups including ethyl and hydroxyethyl (**1d7**, **1d8**, and **1d9**), both of them led to the loss of potency, suggesting that electrostatic interaction has a more dominant role than hydrogen bond in this situation. Starting from **1d4**, we further tested the suitable length of

R^2 group. Compounds **1d10** and **1d11** with *N*-(2-(methylamino)ethyl) and 3-aminopropyl substitutions on the sulfonamide amino group could activate GPX4, while compound **1d12** with 4-aminobutyl substituent was not active. In general, a 2-aminoethyl R^2 group fits the best for the limited space in the allosteric site. Overall, SAR studies supported the predicted binding position of **1** and allowed us to identify compounds that are more potent.

Mutagenesis Studies. We further corroborated the binding positions using site directed mutagenesis. According to the molecular docking structures, the activators interacted with the side chain carboxyl groups of residues D21 and D23 (Figure 4a). We generated two single mutants (D21A and D23A) and one double mutant (D21A/D23A). GPX4 activation by compound **1** and **1d4** was reduced for D21A and D23A and was dramatically deteriorated for D21A/D23A, supporting the predicted hydrogen bond and electrostatic interactions (Figure 4b). The dissociation constant of **1d4** with D21A/D23A was further determined using SPR assay (K_D = 374 ± 8 μM, Supporting Information, Figure S7). The reduced binding to the mutant enzyme also supports the docking positions. Interestingly, the D21A, D23A, and D21A/D23A mutants showed increased enzymatic activities, implying these residues may be involved in regulating GPX4 enzymatic activity. D23 forms salt bridge with K90 in the allosteric site. Activator compound interacting with D23 would weaken the salt bridge, and possibly stabilize the conformation of the catalytic triad (C46, Q81, and W136) favorable for catalysis through the two pathways indicated in Figure 1a. The biological relevance of this finding warrants further investigation.

a)

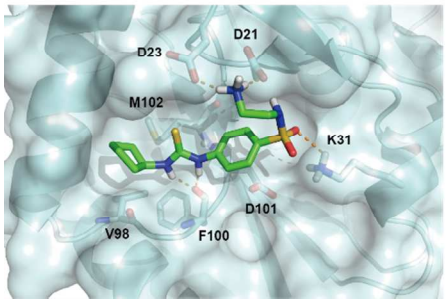

b)

Enzyme	Enzyme activity compared to GPx4 U46C (%)	Conc. required to reach 150% activation[a] (μM)	
		1	**1d4**
U46C	100 ± 1	248	20
D21A, U46C	126 ± 3	618	367
D23A, U46C	113 ± 2	372	235
D21A, D23A, U46C	129 ± 2	> 1000	382

Figure 4. Binding mode of **1d4**. a) Predicted binding mode of **1d4** to GPX4. The hydrogen bonds between the activator (green) and GPX4 (pale cyan) are shown as orange dash lines. b) Enzyme activities and responses to **1** and **1d4** of GPX4 mutants. [a]Data were given by reading corresponding values from the curves fitted by the Hill model. Data shown represent the mean ± SEM (n = 3).

Selectivity Study. Compound **1** and **1d4** were tested in a GPX4-specific activity assay using mouse embryonic fibroblasts (MEF) cell extracts, and both of them activated GPX4 dose-dependently (Figure 5a). The **1d4** concentration required to activate the GPX4 activity to 150 % was 61 μM. To further evaluate the selectivity and specificity of the compounds in a cellular context, we measured GPX4-specific activity in GPX4-knockout mouse embryonic fibroblasts re-constituted with a mouse wild-type GPX4 and a mock transduced control (Figure 5b). In addition, when using cholesterol hydroperoxide (ChOOH, a specific GPX4 substrate) as a stressor, compound **1** and **1d4** could activate GPX4 in intact cells and protect them from ChOOH toxic effects (Figure 5c).

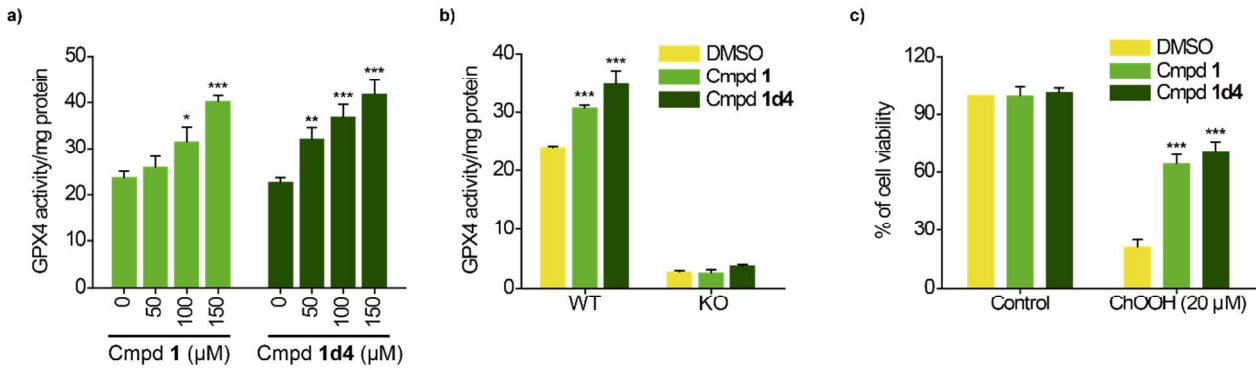

Figure 5. Assessment of the GPX4-specific activity. a) Dose-dependent GPX4 activity assay of **1** and **1d4**. GPX4 specific activity is expressed as NADPH (nmoles) consumed per mg of protein per min. Data shown represent the mean ± s.d. (n = 3). b) Cell extracts were prepared from GPX4 conditional KO MEFs expressing a GPX4 expressing vector (WT) and a mock empty control (KO) to assess the GPX4 specific activity induced by **1** and **1d4** (100 μM). c) Cholesterol hydroperoxide (ChOOH) induced cell death assay. **1** and **1d4** (200 μM) prevented cell death induced by the GPX4 specific substrate ChOOH (20 μM). Data shown represent the mean ± s.d. (n = 4). The statistical significance was determined using a two-tailed t-test, *$p < 0.05$, **$p < 0.01$, ***$p < 0.001$.

CONCLUSION

Despite significant advantages of protein activators, few known small molecule activators exist. Using a structure and computational-based approach, we identified an allosteric site in GPX4 and discovered eight GPX4 allosteric activators. To the best of our knowledge, this is the first report of GPX4 enzyme activators. We also verified that these compounds were not reducing agents or iron chelators (Supporting Information, Figure S8 and Figure S9). These small molecules can

suppress ferroptosis with a mechanism distinct from all other inhibitors described so far. Ferroptosis inhibitors that function by activating the GPX4 enzyme activity are expected to be more specific than the lipid ROS scavenger Ferrostatin/Liproxstatin and iron chelators like deferoxamine and ciclopirox olamine. GPX4 activators do not interfere with cellular iron concentrations or other iron-related physiological processes.

For the eight GPX4 activators, we searched SciFinder for substances with similar structures in related studies. Seven compounds (**1**, **1s1**, **1s3**, **1d3**, **1d4**, **1d10**, and **1d11**) have unique structures not published before. For compound **1s2**, it was reported by Vullo *et al*. as inhibitor of the zinc-containing cancer-associated carbonic anhydrases (CA) isozyme IX, with inhibition constant of 37 nM.[27] To rule out possible interference of zinc-related processes, we confirmed that these GPX4 activators were not zinc chelators (Supporting Information, Figure S10).

In conclusion, we found novel allosteric GPX4 activators using combined computational and experimental approaches. The activators can increase GPX4 activity and produce beneficial outcomes in biological processes involving GPX4, supporting further development of these molecules as promising cyto-protective and anti-inflammatory agents. These compounds are also the first description of small molecules able to suppress ferroptosis through GPX4 activation. Moreover, our study provides a general strategy for the future development of activators for other protein targets.

EXPERIMENTAL SECTION

Compound Synthesis and Characterization. The compounds selected from virtual screen were purchased from SPECS with purity of more than 90 % and for most compounds greater than 95 % (confirmed by SPECS with NMR, LC-MS, or both; data is available on the website

http://www.specs.net/; for our hits, PKUMDL-LC-101, PKUMDL-LC-101-S01, PKUMDL-LC-101-S02, and PKUMDL-LC-101-S03, NMR and LC-MS data are provided in the Supporting Information). Catalog numbers are provided in the Supporting Information Table S1. For the chemical synthesis of the analogues of **1** for SAR study, synthesis reagents and solvents were obtained from J&K Chemical (Beijing, China) and used without further purification. Characterization of the analogues of **1** are provided in the Supporting Information. ^{1}H and ^{13}C NMR spectra were recorded on Bruker (400 MHz) instruments, using $CDCl_3$ or DMSO-d_6 as deuterated solvents and with the residual solvent as the internal reference. For all NMR experiments, the deuterated solvent signal was used as the internal lock. Coupling constants (*J* values) are given in hertz (Hz). Multiplicities of ^{1}H NMR signals are reported as follows: s, singlet; d, doublet; dd, doublet of doublets; dt, doublet of triplets; t, triplet; q, quartet; m, multiplet; br, broad signal. NMR data was analyzed by using MestReNova Software version 11.0. High-resolution mass spectra (HRMS) were acquired on a Bruker-400 M spectrometer using TMS as internal standard. High resolution mass spectra were recorded on a Bruker Apex IV FTMS mass spectrometer using ESI (electrospray ionization). Analytical thin layer chromatography (TLC) was performed on silica gel 60 F254 precoated plates (0.25 mm) from EMD Chemical Inc., and components were visualized by ultraviolet light (254 nm).

General Procedures for Preparation of Substituted 4-Thioureidobenzenesulfonamide. Amine (15 mmol) R^2NH_2 in 250 mL dichloromethane was stirred at 0 °C, 2 mL triethylamine was added, and 2.33 g (10 mmol) 4-acetamidobenzenesulfonyl chloride was added in portions. Remove the reaction to r.t. for another 1 h, evaporated under reduced pressure, the crude was diluted with 50 mL water and 50 mL EtOH, then added 1.60 g (40 mmol) NaOH, the mixture was stirred at reflux for 3 h; Then it was diluted with water adjusting the pH to 7, extracted with

AcOEt. The organic extracts were washed with brine, dried over Na_2SO_4, filtered, and evaporated under reduced pressure. The crude was purified by flash chromatography on silica gel. Afforded 4-amino-*N*-substitutedbenzenesulfonamide. 4-amino-*N*-substitutedbenzenesulfonamide (5 mmol) was dissolved in 20 mL THF, added 5.0 mL H_2O, the mixture was stirred at r.t. for 30 min, then pour into 200 mL ice-water, filtered, the white solid that separated was collected and dried in vacuo afforded 4-isothiocyanato-*N*-substitutedbenzenesulfonamide. 1 mmol 4-isothiocyanato-*N*-substitutedbenzenesulfonamide was dissolved in 5 mL EtOH, 1 mmol R^1NH_2 was added, the mixture was stirred at r.t., the reaction was monitored by TLC until the starting materials disappeared. The product was separated by filtration, dried in vacuo afforded substituted 4-thioureidobenzenesulfonamide. For the *N*-boc protecting group, the final products were obtained by hydrochloric acid. The carbamate was dissolved in 5 mL EtOH, and added 0.5 mL EtOAc-HCl, the mixture was stirred at r.t. for 3 h, filtered, the white solid that separated was collected and dried in vacuo afforded corresponding hydrochloride products.

***N*-(2-Aminoethyl)-4-(3-(4-chlorobenzyl)thioureido)benzenesulfonamide Hydrochloride (1d1).** ^{1}H NMR (400 MHz, DMSO-d_6): δ 10.75 (s, 1H), 9.00 (t, J = 5.8 Hz, 1H), 7.98 (s, 3H), 7.93 – 7.84 (m, 3H), 7.78 – 7.70 (m, 2H), 7.39 (q, J = 8.6 Hz, 4H), 4.76 (d, J = 5.8 Hz, 2H), 2.96 (q, J = 6.3 Hz, 2H), 2.85 (m, 2H). ^{13}C NMR (100 MHz, DMSO-d_6): δ 181.24, 144.30, 138.18, 133.74, 131.91, 129.72, 128.70, 127.80, 121.68, 46.50, 40.51, 38.98. HRMS (ESI): calcd for $C_{16}H_{20}ClN_4O_2S_2^+$, [(M+H)$^+$], 399.0711, found 399.0722.

***N*-(2-Aminoethyl)-4-(3-ethylthioureido)benzenesulfonamide Hydrochloride (1d2).** ^{1}H NMR (400 MHz, DMSO-d_6): δ 10.60 (s, 1H), 8.57 (s, 1H), 8.25 – 7.59 (m, 8H), 3.54 – 3.40 (m, 2H), 3.02 – 2.79 (m, 4H), 1.13 (t, J = 7.2 Hz, 3H). ^{13}C NMR (100 MHz, DMSO-d_6): δ 180.44, 144.51,

133.35, 127.76, 121.22, 40.50, 38.96, 38.88, 14.38. HRMS (ESI): calcd for $C_{11}H_{19}N_4O_2S_2^+$, [(M+H)$^+$], 303.0944, found 303.0943.

***N*-(2-Aminoethyl)-4-(3-(*tert*-butyl)thioureido)benzenesulfonamide Hydrochloride (1d3).** ^{1}H NMR (400 MHz, DMSO-d_6): δ 10.56 (s, 1H), 8.36 (s, 1H), 8.00 (s, 3H), 7.87 (t, J = 8.5 Hz, 3H), 7.69 (d, J = 8.5 Hz, 2H), 3.09 – 2.74 (m, 4H), 1.49 (s, 9H). ^{13}C NMR (100 MHz, DMSO-d_6): δ 179.53, 143.95, 134.65, 127.53, 121.80, 53.49, 44.13, 40.53, 28.82. HRMS (ESI): calcd for $C_{13}H_{23}N_4O_2S_2^+$, [(M+H)$^+$], 331.1257, found 331.1257.

***N*-(2-Aminoethyl)-4-(3-cyclopentylthioureido)benzenesulfonamide Hydrochloride (1d4).** ^{1}H NMR (400 MHz, DMSO-d_6): δ 10.26 (s, 1H), 8.51 (s, 1H), 7.86 (d, J = 8.5 Hz, 4H), 7.80 (t, J = 5.7 Hz, 1H), 7.70 (d, J = 8.8 Hz, 2H), 4.60 – 4.43 (m, 1H), 2.94 (q, J = 6.3 Hz, 2H), 2.85 (q, J = 6.1 Hz, 2H), 1.93 (dt, J = 13.2, 6.5 Hz, 2H), 1.74 – 1.62 (m, 2H), 1.61 – 1.43 (m, 4H). ^{13}C NMR (100 MHz, DMSO-d_6): δ 179.42, 144.21, 139.62, 127.19, 120.41, 54.88, 40.00, 38.48, 31.98, 23.33. HRMS (ESI): calcd for $C_{14}H_{23}N_4O_2S_2$, [(M+H)$^+$], 343.1257, found 343.1262.

***N*-(2-Aminoethyl)-4-(3-cyclohexylthioureido)benzenesulfonamide Hydrochloride (1d5).** ^{1}H NMR (400 MHz, DMSO-d_6): δ 9.96 (s, 1H), 8.17 (s, 1H), 7.84 – 7.73 (m, 4H), 7.68 (d, J = 8.8 Hz, 2H), 7.50 (s, 1H), 4.15 – 4.05 (m, 1H), 3.15 (t, J = 7.0 Hz, 2H), 2.92 (s, 2H), 1.97 – 1.87 (m, 2H), 1.71 (s, 2H), 1.60 – 1.55 (m, 2H), 1.32 – 1.19 (m, 4H). HRMS (ESI): calcd for $C_{15}H_{25}N_4O_2S_2$, [(M+H)$^+$], 357.1415, found 357.1415.

***N*-(2-Aminoethyl)-4-(3-cycloheptylthioureido)benzenesulfonamide Hydrochloride (1d6).** ^{1}H NMR (400 MHz, DMSO-d_6): δ 10.51 (s, 1H), 8.58 (d, J = 8.0 Hz, 1H), 7.95 (s, 3H), 7.90 (d, J = 8.8 Hz, 2H), 7.83 (t, J = 5.9 Hz, 1H), 7.70 (d, J = 8.8 Hz, 2H), 4.28 (m, 1H), 2.95 (q, J = 6.3 Hz, 2H), 2.84 (q, J = 6.3 Hz, 2H), 1.94 – 1.89 (m, 2H), 1.64 – 1.43 (m, 10H). ^{13}C NMR (100 MHz,

DMSO-d_6): δ 179.14, 144.71, 127.70, 120.99, 54.39, 38.98, 34.13, 28.21, 24.11. HRMS (ESI): calcd for $C_{16}H_{27}N_4O_2S_2^+$, [(M+H)$^+$], 371.1570, found 371.1560.

4-(3-Cyclopentylthioureido)-*N*-ethylbenzenesulfonamide (1d7). ^{1}H NMR (400 MHz, DMSO-d_6): δ 9.66 (s, 1H), 8.10 (s, 1H), 7.77 – 7.63 (m, 4H), 7.43 (t, J = 5.7 Hz, 1H), 4.50 (s, 1H), 2.76 (qd, J = 7.2, 5.6 Hz, 2H), 1.95 (dq, J = 12.9, 7.2 Hz, 2H), 1.73 – 1.43 (m, 6H), 0.97 (t, J = 7.2 Hz, 3H). ^{13}C NMR (100 MHz, DMSO-d_6): δ 179.97, 143.96, 127.58, 121.45, 55.68, 37.98, 32.40, 23.86, 15.19. HRMS (ESI): calcd for $C_{14}H_{21}N_3O_2S_2$, [(M+H)$^+$], 328.1153, found 328.1146.

4-(3-Cyclopentylthioureido)-*N*-(2-hydroxyethyl)benzenesulfonamide (1d8). ^{1}H NMR (400 MHz, DMSO-d_6): δ 9.66 (s, 1H), 8.11 (s, 1H), 7.80 – 7.64 (m, 4H), 7.47 (t, J = 6.0 Hz, 1H), 4.68 (t, J = 5.6 Hz, 1H), 4.53 – 4.47 (m, 1H), 3.37 (q, J = 6.2 Hz, 2H), 2.77 (q, J = 6.2 Hz, 2H), 1.99 – 1.91 (m, 2H), 1.72 – 1.41 (m, 8H). ^{13}C NMR (100 MHz, DMSO-d_6): δ 179.97, 143.97, 127.59, 60.38, 55.68, 45.53, 32.39, 23.86. HRMS (ESI): calcd for $C_{14}H_{21}N_3O_3S_2$, [(M+H)$^+$], 344.1097, found 344.1096.

4-(3-(4-Chlorobenzyl)thioureido)-*N*-(2-hydroxyethyl)benzenesulfonamide (1d9). ^{1}H NMR (400 MHz, DMSO-d_6): δ 10.02 (s, 1H), 8.53 (s, 1H), 7.71 (d, J = 3.5 Hz, 4H), 7.51 (t, J = 5.2 Hz, 1H), 7.39 (q, J = 8.7 Hz, 4H), 4.75 (d, J = 5.2 Hz, 2H), 4.69 (t, J = 5.5 Hz, 1H), 3.44 – 3.31 (m, 2H), 2.87 – 2.74 (m, 2H). ^{13}C NMR (100 MHz, DMSO-d_6): δ 181.16, 143.52, 138.20, 135.27, 131.94, 129.79, 128.70, 127.71, 122.27, 60.39, 46.88, 45.55, 40.15, 39.94, 39.73. HRMS (ESI): calcd for $C_{16}H_{18}ClN_3O_3S_2$, [(M+H)$^+$], 400.0551, found 400.0551.

4-(3-Cyclopentylthioureido)-*N*-(2-(methylamino)ethyl)benzenesulfonamide Hydrochloride (1d10). ^{1}H NMR (400 MHz, DMSO-d_6): δ 10.18 (s, 1H), 8.60 (s, 2H), 8.44 (d, J = 7.7 Hz, 1H),

7.86 – 7.82 (m, 3H), 7.76 – 7.65 (m, 2H), 4.55 – 4.45 (m, 1H), 3.00 – 2.95 (m, 5H), 2.54 (t, *J* = 5.2 Hz, 2H), 1.93 (dt, *J* = 13.3, 6.5 Hz, 2H), 1.74 – 1.35 (m, 6H). ^{13}C NMR (100 MHz, DMSO-d_6): δ 180.95, 144.68, 134.80, 126.49, 121.96, 51.17, 48.40, 40.29, 33.39, 30.65, 23.35. HRMS (ESI): calcd for $C_{15}H_{26}N_4O_2S_2^+$, [(M+H)$^+$], 357.1413, found 357.1415.

***N*-(3-Aminopropyl)-4-(3-cyclopentylthioureido)benzenesulfonamide Hydrochloride (1d11).** ^{1}H NMR (400 MHz, DMSO-d_6): δ 10.55 (s, 1H), 8.71 (s, 1H), 8.07 – 7.56 (m, 8H), 4.52-4.47 (m, 1H), 2.82-2.73 (m, 4H), 1.96 – 1.85 (m, 2H), 1.73-1.63 (m, 4H), 1.58-1.43 (m, 4H). ^{13}C NMR (100 MHz, DMSO-d_6): δ 179.90, 144.42, 127.49, 120.86, 55.37, 36.98, 32.49, 27.89, 23.83. HRMS (ESI): calcd for $C_{15}H_{25}N_4O_2S_2^+$, [(M+H)$^+$], 357.1413, found 357.1406.

***N*-(4-Aminobutyl)-4-(3-cyclopentylthioureido)benzenesulfonamide Hydrochloride (1d12).** ^{1}H NMR (400 MHz, DMSO-d_6): δ 10.73 (s, 1H), 8.87 (d, *J* = 23.5 Hz, 1H), 8.15-8.00 (m, 4H), 7.90 (d, *J* = 8.6, 2H), 7.67 (d, *J* = 8.6 Hz, 2H), 4.53 - 4.46 (m, 1H), 3.45 (q, *J* = 6.6 Hz, 2H), 2.70 (t, *J* = 7.0 Hz, 2H), 1.94 – 1.83 (m, 4H), 1.74-1.64 (m, 4H), 1.60 – 1.49 (m, 4H). ^{13}C NMR (100 MHz, DMSO-d_6): δ 179.90, 144.41, 133.97, 127.44, 120.68, 55.25, 51.62, 42.40, 38.74, 31.07, 26.49, 24.71, 23.89. HRMS (ESI): calcd for $C_{16}H_{27}N_4O_2S_2^+$, [(M+H)$^+$], 371.1570, found 371.1564.

Reagents and Cell Culture. Reagents were purchased from Sigma-Aldrich unless otherwise noted. The pQE-30 bacterial expression plasmid of the U46C mutant of human cytosolic GPX4 was a generous gift from Professor Hartmut Kuhn (University Medicine Berlin-Charité, Germany). IPTG, PMSF, DTT, EDTA, and glutathione were from Amresco. Standard compounds for LC-MS/MS were purchased from Cayman Chemical. Calcium ionophore A23187 was obtained from J&K Chemical. The Symmetry C18 reverse-phase column (3.5 µm,

2.1 mm × 150 mm) was purchased from Waters Corp. HT-1080 cells were the generous gift of Professor Chu Wang (Peking University, China). HEK293T cells were received as a gift from Professor Jincai Luo (Peking University, China). The Dual-Glo Luciferase Assay System was from Promega. ChOOH was a kind gift of Prof. Sayuri Myiamoto (Universidade de Sao Paulo, Brazil).

Allosteric Site Prediction and Virtual Screen. Potential allosteric site in GPX4 was identified using the CAVITY and CorrSite program[16,17,19], and then applied to screen for potential allosteric modulator. The volume of the predicted allosteric site is smaller than the substrate site (278.4 $Å^3$ versus 407.5 $Å^3$), but their predicted maximal pKds (an index for ligandability assessment of binding cavities, depending on the volume, lip size, hydrophobic volume, surface area, and hydrogen-bond forming surface area of the cavity) are comparable (7.48 versus 7.82). Rigid body docking was first performed with default parameters using the molecular docking program Glide in SP mode[28,29], to screen the SPECS compounds library (May 2013 version for 10 mg; 197,276 compounds). Flexible ligands and rigid receptor docking was then performed using the Glide XP mode with default parameters to further screen the top 10,000 compounds from the SP results. After this, the binding conformations of the top 2,000 compounds from Glide XP were exported and manually selected. Finally, 251 compounds were purchased for experimental testing. Correlation analysis between experimental pEC_{50} and calculated pK_d is given in Supporting Information, Figure S11 and Table S2.

Protein Expression and Purification. The recombinant mutant plasmid was transformed to *Escherchia coli* strain M15. Recombinant cells were cultivated at 37 °C in LB medium containing kanamycin (25 μg/mL) and ampicillin (100 μg/mL). At an OD_{600} of 0.6, GPX4 expression was induced by addition of IPTG (1 mM) and the cells were further cultured at 30 °C

for 5 h. The cells were harvested by centrifugation (6,000 rpm, 15 min), resuspended in lysis buffer [Tris-HCl (100 mM, pH 8.0), NaCl (300 mM), imidazole (20 mM), TCEP (5 mM), and PMSF (1 mM)] and incubated on ice with 1 mg/mL lysozyme for 30 min. After sonication, the lysate was centrifuged (17,000 rpm, 40 min) and the supernatant was purified using a nickel−nitrilotriacetic acid column (HisTrap HP; GE Healthcare) at 4 °C. The his-tagged GPX4 was eluted with an increasing imidazole step-gradient (100-250 mM). The eluted enzyme was further subject to dialysis for 12 h [Tris-HCl (100 mM, pH 7.4), DTT (1 mM), and glycerol (20 % v/v)] to remove the bulk of imidazole. The final purity of the enzyme was more than 95 % as confirmed by SDS−PAGE. Protein concentrations were measured using Nanodrop 2000 (Thermo Scientific, USA).

Activation of GPX4 in a Cell-Free Assay. By coupling the oxidation of NADPH to $NADP^+$ by oxidized glutathione in the presence of glutathione reductase, GPX4 activity was assessed by measuring the decrease in NADPH fluorescence emission at 460 nm (excitation at 335 nm). To evaluate the effects of compounds on GPX4 activity, compounds were first pre-incubated with purified GPX4 mutants in the assay buffer [Tris-HCl (100 mM, pH 7.4), EDTA (5 mM), Triton X-100 (0.1 % v/v), NADPH (0.2 mM), glutathione (3 mM), and glutathione reductase (1 unit)] for 5 min at 37 °C. Then the reaction was initiated by adding *tert*-butyl hydroperoxide (25 μM). Each compound was dissolved in DMSO at a final concentration of 5 %, which did not perturb the assay. Fluorescence signals were recorded for 6 min on a plate reader (Synergy, BioTek). The initial reaction rates at different concentrations of compound were used to determine EC_{50} values, which were calculated with a four-parameter logistical model of log dose against percentage activation or inhibition and were obtained from at least three sets of experiments. Assay system without adding GPX4 was used to exclude the influence of the redox properties of

compounds. Control experiments were also conducted to confirm that the compounds were not glutathione reductase activators or inhibitors.

SPR Experiments. The binding affinities of compounds towards GPX4 were assayed using the SPR-based Biacore T200 instrument (GE Healthcare, Uppsala, Sweden). GPX4 was immobilized on a CM5 sensor chip by using standard amine-coupling at 25 °C with running buffer PBS-P [phosphate buffer (20 mM, pH 7.4), NaCl (2.7 mM), KCl (137 mM), surfactant P-20 (0.05 %)] as described previously.[30] A reference flow cell was activated and blocked in the absence of GPX4. In the direct binding experiments between GPX4 and compounds, GPX4 immobilization level was fixed at 800 response units (RU), and then different concentrations of compounds containing 5 % DMSO were serially injected into the channel to evaluate binding affinity. Regeneration was achieved by extended washing with the running buffer after each sample injection. The equilibrium dissociation constants (K_D) of the compounds were obtained by fitting binding response units to Hill equation.

Prevention of Erastin-Induced Ferroptosis by GPX4 Activator in HT-1080 Cells. HT-1080 cells were cultured in DMEM containing 10 % FBS, 1 % supplemented non-essential amino acids and 1 % Pen-Strep mixture (all from Gibco) and maintained in a humidified atmosphere with 5 % CO_2 at 37 °C. The day before the experiment, 2,000 cells/well were seeded in 96-well plates (Corning). The day of the experiment, the medium was changed to fresh DMEM containing different concentrations of GPX4 activator. After 30 min incubation at 37 °C in a tissue culture incubator, erastin (10 μM) was added to stimulate ferroptosis. After 24 hours, cell viability was determined by MTS assay according to the instructions of the CellTiter 96® AQ_{ueous} One Solution Cell Proliferation Assay System (Promega). In brief, 10 μL CellTiter 96® AQ_{ueous} One Solution Reagent was added to each well. Then cells were incubated at 37 °C for 1-

4 hours in a humidified, 5 % CO_2 atmosphere. After incubation, the absorbance at 490 nm was recorded with a BioTek synergy 4 Multi-Mode Microplate Reader. The background absorbance was subtracted from all reported measures. In addition to MTS assay, cell viability was assessed by trypan blue exclusion test (Supporting Information, Figure S12).

Influence of the GPX4 Activator in Human Polymorphonuclear Leucocytes. Following the reported procedure,[3] human PMN cells were isolated from the venous blood of healthy volunteers who had not received non-steroidal anti-inflammatory drugs (NSAIDs) for at least 14 days. Informed consent for participation was obtained from all the volunteers. PMNs were pre-incubated with vehicle (DMSO) and GPX4 activator at 37 °C for 15 min, respectively. To stimulate the PMNs, 10 μM A23187, 2 mM $CaCl_2$, and 500 μM $MgCl_2$ were added. After incubation for 120 min at 37°C, reactions were terminated by the addition of cold methanol (700 μL of methanol was added into 300 μL of reaction solution). 15(S)-HETE-d_8 and PGB_2 were added as internal standards. The upper solvent was evaporated under a stream of nitrogen, and the residue was dissolved in 150 μL of methanol before LC-MS analysis.

LC-MS/MS Method. LC separation was performed with a Shimadzu Prominence UFLC XR (Shimadzu Corporation). The multiple-reaction-monitoring (MRM) spectra were obtained with a QTRAP 5500 mass spectrometer (AB SCIEX) equipped with an ESI source. A Waters Symmetry reverse-phase C18 column (2.1 mm × 150 mm, 3.5 μm) was used for the LC separation as described.[15] Up to 35 eicosanoids and two internal standards [15(S)-HETE-d_8 and PGB_2] were monitored. Optimized LC-MS/MS parameters for the analysis of eicosanoids are in accordance with previous research.[15]

Inhibition of COX-1 and COX-2 in a Cell-Free Assay. COXs can convert AA to PGG_2, and further reduce PGG_2 to PGH_2. The enzyme activities of COXs were determined spectrophotometrically by monitoring the oxidation of *N,N,N',N'*-tetramethyl-*p*-phenylenediamine (TMPD) at 610 nm during the conversion of PGG_2 to PGH_2. The test compound was pre-incubated with purified COX-1 or COX-2 for 15 min. Next, TMPD solution was added, and the reaction was initiated by adding a solution of AA. Absorbance at 610 nm was recorded on a plate reader (Synergy, BioTek). Inhibition activities were measured as described.[31]

Inhibition of mPGES-1 in a Cell-Free Assay. The enzyme activity of mPGES-1 was measured by assessment of PGH_2 conversion to PGE_2.[32] The test compound was pre-incubated with enzyme sample for 15 min. Next, PGH_2 was added to start the reaction. After 1 min, stop solution was added to terminate the reaction. Production of PGE_2 in the reaction mixture was measured with the PGE_2 EIA kit (Cayman Chemical). Inhibition was measured in a similar manner as that of GPX4.

Inhibition of 5-LOX in a Cell-Free Assay. The enzyme activity of 5-LOX was determined spectrophotometrically by monitoring the oxidation of H_2DCFDA to the highly fluorescent 2',7'-dichlorofluorescein during the catalytic reaction mediated by 5-LOX as reported.[33] The test compound was pre-incubated with enzyme for 10 min. Next, the reaction was initiated by the addition of AA, and fluorescence signals (excitation at 500 nm and emission at 520 nm) were recorded on a plate reader (Synergy, BioTek). The human 5-LOX protein was prepared as previous reported.[34]

Inhibition of LTA_4H in a Cell-Free Assay. LTA_4H hydrolase activity was measured by monitoring the formation of LTB_4 with an enzyme-linked immunosorbent assay. The test

compound was pre-incubated with enzyme for 15 min. Next, LTA_4 was added to initiate the reaction. After 10 min, the reaction mixture was diluted to stop the reaction, and the production of LTB_4 was measured with the LTB_4 ELISA kit (Cayman Chemical). Inhibition activities were measured as described.[35]

Activation and Inhibition of 12-LOX and 15-LOX in a Cell-Free Assay. The enzyme activities of 12-LOX and 15-LOX were assessed spectrophotometrically by measuring the formation of 12-HpETE and 15-HpETE, respectively. The test compound was pre-incubated with the enzyme for 1 min. Next, AA was added to initiate the reaction. Absorbance of product at 235 nm was monitored on a plate reader (Synergy, BioTek). Activation or Inhibition activities were measured as described.[15]

Inhibition of the NF-κB Pathway by GPX4 Activator in Luciferase Activity Assay. All plasmid DNAs were prepared using the TIANprep Mini Plasmid Kit (TIANGEN). HEK293T cells were grown to 70 % confluency in 96-well plates (Corning) at 37 °C in DMEM supplemented with 10 % FBS, and treated with Entranster™-H (Engreen) transfection reagent (0.1 μL) and purified plasmids [0.25 μg pGL4.74(hRluc/TK) and 0.25 μg pGL4.32(luc2P/NF-κB-RE/Hygro plasmid)] in 50 μL DMEM/10 % FBS per well. 24 hours later, GPX4 activator was incubated with the cells (2×10^5 cells per well) for 30 min. After incubation, TNFα (5 ng/mL) or IL-1β (10 ng/mL) was added to stimulate the cells for 6 h or 24 h, respectively. Then the luciferase assays were carried out using the Dual-Glo Luciferase Assay System (Promega) with a BioTek synergy 4 Multi-Mode Microplate Reader.

Mutagenesis Experiments. All mutagenesis experiments were carried out according to the instructions of the QuikChange Site-Directed Mutagenesis (SBS Genetech Co., Ltd, Beijing,

China). The pQE-30 bacterial expression plasmid of the U46C mutant of human cytosolic GPX4 was mutated to obtain the mutants. The DNA sequences of all mutants were verified by DNA sequencing. The protein expression and activity assays of the mutants were performed as described for the U46C mutant.

GPX4-Specific Activity Assay. GPX4-specific activity was measured in GPX4 KO MEFs re-constituted with a mouse WT GPX4 (WT) and a mock transduced control (KO). All cell lines were cultured in the presence of α-Toc (10 μM) as this would allow the KO cells to proliferate as previously described.[36] GPX4 specific activity was carried out in a coupled assay, by monitoring the consumption of NADPH in the presence of glutathione reductase upon addition of phosphatidyl choline hydroperoxide.[37]

Viability Assay. Cells were seeded onto 96-well plates (5,000 cells per well) and allowed to attach overnight. The next day, the cells were pre-treated for one hour with the different GPX4 activators at a fixed concentration (200 μM). Upon that medium was changed and cells were exposed to 20 μM ChOOH. After 24 hours viability was assessed using the AquaBluer assay as previously described.[7]

Testing of Reducing Effects. The stable radical 2,2-diphenyl-1-picrylhydrazyl (DPPH) assay[6] was used for the testing. The antioxidant trolox was used as the positive control.

Iron Chelating Ability Assay. The Prussian blue assay was used for the testing. The iron chelators deferoxamine (DFO), ciclopirox olamine (CPX), and EDTA were used as the positive control. 50 μL of each test compound dissolved in DMSO (10 mM) was added to 50 μL of $FeSO_4$ (3 mM) and incubated for 10 min. After incubation, 50 μL of $K_3[Fe(CN)_6]$ (2 mM) was

added and the absorbance at 680 nm was recorded with a BioTek synergy 4 Multi-Mode Microplate Reader.

Zinc Chelating Ability Assay. Zinc reacts with thiocyanate and crystal violet to form a ternary ion-association complex, with maximum absorption at 522 nm. The zinc chelators EDTA and thiourea were used as the positive control. 50 μL of each test compound dissolved in DMSO (10 mM) was added to 50 μL of $ZnSO_4$ (2.5 mM) and incubated for 10 min. After incubation, 50 μL of crystal violet (5 mg/mL) and 100 μL of NH_4SCN (0.25g/mL) were added and the absorbance at 522 nm was recorded with a BioTek synergy 4 Multi-Mode Microplate Reader.

ASSOCIATED CONTENT

Supporting Information

The following files are available free of charge.

Figures S1-S12, Table S1, and spectra of compounds (PDF)

Docked complexes of GPX4 with compound **1** and **1d4** (PDB)

Molecular formula strings (CSV)

AUTHOR INFORMATION

Corresponding Authors

*E-mail: lhlai@pku.edu.cn.

*E-mail: pedro.angeli@virchow.uni-wuerzburg.de.

Author Contributions

C.L. and X.D. have equal contributions of this work.

L.L. and C.L. conceived the project. C.L. performed allosteric site prediction and virtual screen, protein expression and purification, enzymatic assays, SPR experiments, cell-based assays, and mutagenesis. X.D. performed chemical synthesis and purity analysis of the compounds. X.D. and Y.L. contributed to the SAR study. J.P.F.A. and M.C. provided reagents, conducted GPX4-specific activity assay and ChOOH viability assay. W.Z. performed molecular dynamics simulations. X.X. participated in cell-free assay of GPX4 and cell experiments. C.L., X.D., J.P.F.A., and L.L. wrote the manuscript.

Notes

The authors declare no competing financial interest.

ACKNOWLEDGMENT

This work was supported in part by the Ministry of Science and Technology (2016YFA0502303, 2015CB910300 to L.L.), the National Natural Science Foundation of China (21633001 to L.L.), the Rudolf Virchow Jr group leader program from the University of Würzburg (JPFA) and the Human Frontier Science Program (HFSP) (RGP0013 to M.C.). The authors acknowledge Dr. H. Kuhn (University Medicine Berlin-Charité) for sharing the GPX4 bacterial expression plasmid and Mrs Irina Ingold (Helmholtz Zentrum München) for the generation of phosphatidyl choline hydroperoxide.. We thank Dr. C. Wang (Peking University) for helpful discussions and for providing the HT-1080 cells. We also appreciate Dr. J. Zhao (Peking University) for help with cell culture and discussions.

ABBREVIATIONS

AA, arachidonic acid; ACSL4, acyl-CoA synthetase long-chain family member 4; ChOOH, cholesterol hydroperoxide; COX-1, cyclooxygenase 1; COX-2, cyclooxygenase 2; CPX,

ciclopirox olamine; DFO, deferoxamine; Era, erastin; GPX4, glutathione peroxidase 4; hGPX4-C, human GPX4 U46C mutant; LOX, lipoxygenase; LTA_4H, leukotriene A4 hydrolase; LTB_4, leukotriene B_4; MEF, mouse embryonic fibroblasts; mPGES-1, microsomal prostaglandin E_2 synthase 1; PMN, human polymorphonuclear leucocytes; SAR, structure-activity relationship; SPR, surface plasmon resonance.

REFERENCES

(1) Brigelius-Flohé, R. Glutathione peroxidases and redox-regulated transcription factors. *Biol. Chem.* **2006**, *387*, 1329−1335.

(2) Yang, W. S.; SriRamaratnam, R.; Welsch, M. E.; Shimada, K.; Skouta, R.; Viswanathan, V. S.; Cheah, J. H.; Clemons, P. A.; Shamji, A. F.; Clish, C. B.; Brown, L. M.; Girotti, A. W.; Cornish, V. W.; Schreiber, S. L.; Stockwell, B. R. Regulation of ferroptotic cancer cell death by GPX4. *Cell* **2014**, *156*, 317−331.

(3) Yang, K.; Ma, W.; Liang, H.; Ouyang, Q.; Tang, C.; Lai, L. Dynamic simulations on the arachidonic acid metabolic network. *PLoS Comput. Biol.* **2007**, *3*, e55.

(4) Yang, K.; Bai, H.; Ouyang, Q.; Lai, L.; Tang, C. Finding multiple target optimal intervention in disease-related molecular network. *Mol. Syst. Biol.* **2008**, *4*, 228.

(5) Meng, H.; Liu, Y.; Lai, L. H. Diverse ways of perturbing the human arachidonic acid metabolic network to control inflammation. *Acc. Chem. Res.* **2015**, *48*, 2242−2250.

(6) Dixon, S. J.; Lemberg, K. M.; Lamprecht, M. R.; Skouta, R.; Zaitsev, E. M.; Gleason, C. E.; Patel, D. N.; Bauer, A. J.; Cantley, A. M.; Yang, W. S.; Morrison, B.; Stockwell, B. R. Ferroptosis: an iron-dependent form of nonapoptotic cell death. *Cell* **2012**, *149*, 1060−1072.

(7) Friedmann Angeli, J. P.; Schneider, M.; Proneth, B.; Tyurina, Y. Y.; Tyurin, V. A.; Hammond, V. J.; Herbach, N.; Aichler, M.; Walch, A.; Eggenhofer, E.; Basavarajappa, D.;

Rådmark, O.; Kobayashi, S.; Seibt, T.; Beck, H.; Neff, F.; Esposito, I.; Wanke, R.; Förster, H.; Yefremova, O.; Heinrichmeyer, M.; Bornkamm, G. W.; Geissler, E. K.; Thomas, S. B.; Stockwell, B. R.; O'Donnell, V. B.; Kagan, V. E.; Schick, J. A.; Conrad, M. Inactivation of the ferroptosis regulator Gpx4 triggers acute renal failure in mice. *Nat. Cell Biol.* **2014**, *16*, 1180−1191.

(8) Conrad, M.; Angeli, J. P.; Vandenabeele, P.; Stockwell, B. R. Regulated necrosis: disease relevance and therapeutic opportunities. *Nat. Rev. Drug Discov.* **2016**, *15*, 348−366.

(9) Kagan, V. E.; Mao, G.; Qu, F.; Angeli, J. P.; Doll, S.; Croix, C. S.; Dar, H. H.; Liu, B.; Tyurin, V. A.; Ritov, V. B.; Kapralov, A. A.; Amoscato, A. A.; Jiang, J. F.; Anthonymuthu, T.; Mohammadyani, D.; Yang, Q.; Proneth, B.; Klein-Seetharaman, J.; Watkins, S.; Bahar, H.; Greenberger, J.; Mallampalli, R. K.; Stockwell, B. R.; Tyurina, Y. Y.; Conrad, M.; Bayir, H. Oxidized arachidonic and adrenic PEs navigate cells to ferroptosis. *Nat. Chem. Biol.* **2017**, *13*, 81−90.

(10) Zilka, O.; Shah, R.; Li, B.; Friedmann Angeli, J. P.; Griesser, M.; Conrad, M.; Pratt, D. A. On the mechanism of cytoprotection by ferrostatin-1 and liproxstatin-1 and the role of lipid peroxidation in ferroptotic cell death. *ACS Cent. Sci.* **2017**, *3*, 232−243.

(11) Doll, S.; Proneth, B.; Tyurina, Y. Y.; Panzilius, E.; Kobayashi, S.; Ingold, I.; Irmler, M.; Beckers, J.; Aichler, M.; Walch, A.; Prokisch, H.; Trumbach, D.; Mao, G. W.; Qu, F.; Bayir, H.; Fullekrug, J.; Scheel, C. H.; Wurst, W.; Schick, J. A.; Kagan, V. E.; Angeli, J. P. F.; Conrad, M. ACSL4 dictates ferroptosis sensitivity by shaping cellular lipid composition. *Nat. Chem. Biol.* **2017**, *13*, 91−98.

(12) Yang, W. S.; Kim, K. J.; Gaschler, M. M.; Patel, M.; Shchepinov, M. S.; Stockwell, B. R. Peroxidation of polyunsaturated fatty acids by lipoxygenases drives ferroptosis. *Proc. Natl. Acad. Sci. USA* **2016**, *113*, E4966−4975.

(13) McCarthy, A. R.; Hollick, J. J.; Westwood, N. J. The discovery of nongenotoxic activators of p53: building on a cell-based high-throughput screen. *Semin. Cancer Biol.* **2010**, *20*, 40−45.

(14) Zorn, J. A.; Wells, J. A. Turning enzymes on with small molecules. *Nat. Chem. Biol.* **2010**, *6*, 179−188.

(15) Meng, H.; McClendon, C. L.; Dai, Z.; Li, K.; Zhang, X.; He, S.; Shang, E.; Liu, Y.; Lai, L. Discovery of novel 15-lipoxygenase activators to shift the human arachidonic acid metabolic network toward inflammation resolution. *J. Med. Chem.* **2016**, *59*, 4202−4209.

(16) Yuan, Y.; Pei, J.; Lai, L. LigBuilder 2: a practical de novo drug design approach. *J. Chem. Inf. Model.* **2011**, *51*, 1083−1091.

(17) Yuan, Y.; Pei, J.; Lai, L. Binding site detection and druggability prediction of protein targets for structure-based drug design. *Curr. Pharm. Des.* **2013**, *19*, 2326−2333.

(18) Scheerer, P.; Borchert, A.; Krauss, N.; Wessner, H.; Gerth, C.; Höhne, W.; Kuhn, H. Structural basis for catalytic activity and enzyme polymerization of phospholipid hydroperoxide glutathione peroxidase-4 (GPx4). *Biochemistry* **2007**, *46*, 9041−9049.

(19) Ma, X.; Meng, H.; Lai, L. Motions of allosteric and orthosteric ligand-binding sites in proteins are highly correlated. *J. Chem. Inf. Model.* **2016**, *56*, 1725−1733.

(20) Baell, J. B.; Holloway, G. A. New substructure filters for removal of pan assay interference compounds (PAINS) from screening libraries and for their exclusion in bioassays. *J. Med. Chem.* **2010**, *53*, 2719−2740.

(21) Buczynski, M. W.; Dumlao, D. S.; Dennis, E. A. An integrated omics analysis of eicosanoid biology. *J. Lipid. Res.* **2009**, *50*, 1015−1038.

(22) Frohberg, P.; Drutkowski, G.; Wobst, I. Monitoring eicosanoid biosynthesis via lipoxygenase and cyclooxygenase pathways in human whole blood by single HPLC run. *J. Pharm. Biomed.* **2006**, *41*, 1317−1324.

(23) Sud'ina, G. F.; Pushkareva, M. A.; Shephard, P.; Klein, T. Cyclooxygenase (COX) and 5-lipoxygenase (5-LOX) selectivity of COX inhibitors. *Prostaglandins Leukotrienes Essent. Fatty Acids* **2008**, *78*, 99−108.

(24) Morgan, M. J.; Liu, Z. G. Crosstalk of reactive oxygen species and NF-κB signaling. *Cell Res.* **2011**, *21*, 103−115.

(25) Brigelius-Flohé, R.; Friedrichs, B.; Maurer, S.; Schultz, M.; Streicher, R. Interleukin-1-induced nuclear factor κB activation is inhibited by overexpression of phospholipid hydroperoxide glutathione peroxidase in a human endothelial cell line. *Biochem. J.* **1997**, *328*, 199−203.

(26) Heirman, I.; Ginneberge, D.; Brigelius-Flohé, R.; Hendrickx, N.; Agostinis, P.; Brouckaert, P.; Rottiers, P.; Grooten, J. Blocking tumor cell eicosanoid synthesis by GPx4 impedes tumor growth and malignancy. *Free Radic. Biol. Med.* **2006**, *40*, 285−294.

(27) Vullo, D.; Steffansen, B.; Brodin, B.; Supuran, C. T.; Scozzafava, A.; Nielsen, C. U. Carbonic anhydrase inhibitors: transepithelial transport of thioureido sulfonamide inhibitors of the cancer-associated isozyme IX is dependent on efflux transporters. *Bioorg. Med. Chem.* **2006**, *14*, 2418−2427.

(28) Friesner, R. A.; Banks, J. L.; Murphy, R. B.; Halgren, T. A.; Klicic, J. J.; Mainz, D. T.; Repasky, M. P.; Knoll, E. H.; Shelley, M.; Perry, J. K.; Shaw, D. E.; Francis, P.; Shenkin, P. S.

Glide: a new approach for rapid, accurate docking and scoring. 1. method and assessment of docking accuracy. *J. Med. Chem.* **2004**, *47*, 1739−1749.

(29) Halgren, T. A.; Murphy, R. B.; Friesner, R. A.; Beard, H. S.; Frye, L. L.; Pollard, W. T.; Banks, J. L. Glide: a new approach for rapid, accurate docking and scoring. 2. enrichment factors in database screening. *J. Med. Chem.* **2004**, *47*, 1750−1759.

(30) Wang, Q.; Qi, Y.; Yin, N.; Lai, L. Discovery of novel allosteric effectors based on the predicted allosteric sites for Escherichia coli D-3-phosphoglycerate dehydrogenase. *PLoS One* **2014**, *9*, e94829.

(31) Chen, Z.; Wu, Y.; Liu, Y.; Yang, S.; Chen, Y.; Lai, L. Discovery of dual target inhibitors against cyclooxygenases and leukotriene A_4 hydrolyase. *J. Med. Chem.* **2011**, *54*, 3650−3660.

(32) He, S.; Li, C.; Liu, Y.; Lai, L. Discovery of highly potent microsomal prostaglandin E_2 synthase 1 inhibitors using the active conformation structural model and virtual screen. *J. Med. Chem.* **2013**, *56*, 3296−3309.

(33) Pufahl, R. A.; Kasten, T. P.; Hills, R.; Gierse, J. K.; Reitz, B. A.; Weinberg, R. A.; Masferrer, J. L. Development of a fluorescence-based enzyme assay of human 5-lipoxygenase. *Anal. Biochem.* **2007**, *364*, 204−212.

(34) Wu, Y.; He, C.; Gao, Y.; He, S.; Liu, Y.; Lai, L. Dynamic modeling of human 5-lipoxygenase-inhibitor interactions helps to discover novel inhibitors. *J. Med. Chem.* **2012**, *55*, 2597−2605.

(35) Jiang, X.; Zhou, L.; Wei, D.; Meng, H.; Liu, Y.; Lai, L. Activation and inhibition of leukotriene A_4 hydrolase aminopeptidase activity by diphenyl ether and derivatives. *Bioorg. Med. Chem. Lett.* **2008**, *18*, 6549−6552.

(36) Seiler, A.; Schneider, M.; Förster, H.; Roth, S.; Wirth, E. K.; Culmsee, C.; Plesnila, N.; Kremmer, E.; Rådmark, O.; Wurst, W.; Bornkamm, G. W.; Schweizer, U.; Conrad, M. Glutathione peroxidase 4 senses and translates oxidative stress into 12/15-lipoxygenase dependent- and AIF-mediated cell death. *Cell Metab.* **2008**, *8*, 237−248.

(37) Roveri, A.; Maiorino, M.; Ursini, F. Enzymatic and immunological measurements of soluble and membrane-bound phospholipid-hydroperoxide glutathione peroxidase. *Methods Enzymol.* **1994**, *233*, 202−212.

Table of Contents graphic.